Ultrawideband through-the-wall propagation

A. Muqaibel, A. Safaai-Jazi, A. Bayram, A.M. Attiya and S.M. Riad

Abstract: The propagation of ultrawideband (UWB) signals in indoor environments is an important issue with significant impacts on the future direction and scope of UWB technology. The propagation of UWB signals is governed, among other things, by the properties of materials in the propagation medium. The information on electromagnetic properties of construction materials in the UWB frequency range would provide valuable insights into the appreciation of the capabilities and limitations of UWB technology. Although electromagnetic properties of certain construction materials over relatively narrow bandwidths in GHz frequency ranges are available, ultrawideband characterisation of most typical construction materials for UWB communication purposes has not been reported. In narrowband wireless communications, only the magnitude of insertion loss has been the quantity of interest. But for UWB signals, in addition to the magnitude, the phase information is an equally important factor that needs to be accounted for. In fact, UWB signals not only suffer attenuation when propagating through walls, but also suffer distortion due to the dispersive properties of the walls. This research examines propagation through typical construction materials and their ultrawideband characterisation. Ten commonly used construction materials are chosen for this investigation. Results for the dielectric constant and loss tangent of the materials over the UWB frequency range are presented. Accuracy of the measured results is discussed and distortions of UWB signals due to the dispersive properties of wall materials are addressed.

1 Introduction

Ultrawideband (UWB) wireless communication has been the subject of extensive investigation in recent years due to its potential applications in high-rate data transmission and its unique capabilities. However, many important aspects of UWB-based communication systems have not yet been thoroughly examined. The propagation of UWB signals in indoor environment is an important issue with significant impacts on the future direction, scope and general extent of the success of UWB technology. At a fundamental level, the propagation of UWB signals, as for any electromagnetic wave, is governed, among other things, by the properties of materials in the propagation medium. The information on electromagnetic properties of building materials in the UWB frequency range (3.1–10.6 GHz) would provide valuable insights into the appreciation of the capabilities and limitations of UWB technology for indoor and indoor–outdoor applications.

Many researchers have studied the propagation of electromagnetic waves through walls and floors. In a review paper, Hashemi [1] summarised much of the earlier investigations on electromagnetic characterisation of building materials. During the past decade, many more investigations on evaluating electrical properties of various building materials over different frequency ranges have been carried out. Zhang and Hwang [2] measured the penetration loss of reinforced concrete and plasterboard walls over the frequency range 900 MHz–18 GHz, while Landron *et al.* [3] examined reflection coefficients at 1.9 GHz and 4.0 GHz for walls made of limestone blocks, glass and brick. In another study, Suzuki and Mohan [4], as part of their investigation of high-resolution indoor channel characteristics, measured the dielectric constant and conductivity of brick and concrete over a bandwidth of 200 MHz centred at 1 GHz. Kharkovsky *et al.* [5] measured the reflection and transmission coefficients of cement-based materials over the X-band (8–12 GHz) frequency range under different curing conditions, while Cuinas and Sanchez [6] carried out characterisation of several building materials, including brick, glass, plasterboard, chipwood, door and façade at 5.8 GHz. More recently, Pena *et al.* [7] reported the permittivity and conductivity of brick and doubly reinforced concrete walls for the 900 MHz band. Extensive data on dielectric properties of a variety of glasses [8] and wood and wood-based materials [9], largely at frequencies outside the UWB range, have also been tabulated.

It is noted from the past work cited above that the available information on building material properties are largely over narrowband frequencies and often limited to one or two materials. In all narrowband measurements, only the magnitude of insertion transfer function (i.e. insertion loss) has been the quantity of interest. But for UWB signals, as in ground penetrating radars, in addition to the magnitude, the phase information is an equally important factor that needs to be accounted for in studying the propagation effects [10]. In fact, UWB signals not only suffer attenuation as in the case of narrowband signals when propagating through walls, but also suffer distortion due to the dispersive properties of the walls. Therefore, narrowband measurements, although helpful in providing some general understanding, are not adequate for UWB propagation analyses, simulations and channel modelling.

The aim of this paper is to examine propagation through walls, which are made of typical building materials and

IEE Proceedings online no. 20050092

doi:10.1049/ip-map:20050092

Paper first received 24th April and in revised form 7th July 2005

The authors are with the Time-Domain and RF Measurement Laboratory, Bradley Department of Electrical and Computer Engineering, Virginia Polytechnic Institute and State University, Blacksburg VA 24061-0111, USA

E-mail: muqaibel@kfupm.edu.sa

thereby acquire ultrawideband characterisation of these materials. The complex dielectric constant of each material and their variations against frequency over the UWB frequency are presented. The results of this investigation provide valuable insights into the transient behaviour of subnanosecond pulses as they propagate through typical construction materials and structures. Ten commonly used construction materials are chosen for this investigation. These include drywall, cloth office partition, structure wood, wooden door, plywood, glass, styrofoam, brick wall, concrete-block wall and reinforced concrete pillar.

Material characterisation can be performed using different techniques, including capacitor, waveguide resonator and coaxial cavity methods, and radiated measurement techniques. Afsar *et al.* [11] presented a detailed review of material characterisation techniques covering a frequency range 1 MHz–1500 GHz. More recently, Baker–Jarvis *et al.* [12] have compared various techniques used for dielectric characterisation of low-loss materials. Radiated measurements are used in this work as they lend themselves to nondestructive and broadband applications. Results for the loss tangent and the dielectric constant of the materials over the UWB frequency range are presented. Both frequency-domain and time-domain measurement techniques are used to validate the results and ensure better accuracy by capitalising on the advantages of each technique.

2 Measurement setup and procedures

The real and imaginary parts of the complex dielectric constant of a material are evaluated through the measurement of an insertion transfer function, defined as the ratio of two frequency-domain signals measured in the presence and in the absence of the material under test. Figure 1 illustrates the schematic diagram of the measurement setup. The measurements may be performed in either the time domain using short duration pulses, or in the frequency domain using sinusoidal signals. The transmitter and receiver antennas are kept at fixed locations and aligned for maximum reception. The material to be measured is placed at nearly the midpoint between the two antennas. The distance between the antennas should be sufficiently large so that the material is in the far field of each antenna. With this arrangement, the electromagnetic field incident on the material is essentially a plane wave. The material under test is assumed to be in the form of a slab with thickness d and held in position such that the plane wave is normally incident on the slab, as depicted in Fig. 1. After the measurement system is prepared, initially the reference time-domain signal $v_t^{fs}(t)$ is measured with a sampling oscilloscope or the reference frequency-domain signal $V_t^{fs}(j\omega)$ is measured with a network analyser in the absence of the material. Then, the time-domain signal $v_t(t)$ or the frequency-domain signal $V_t(j\omega)$ is measured with the material slab in place. The insertion transfer function is calculated as

$$H(j\omega) = \frac{FFT(v_t(t))}{FFT\left(v_t^{fs}(t)\right)} = \frac{V_t(j\omega)}{V_t^{fs}(j\omega)} \quad (1)$$

where $\omega = 2\pi f$ is the angular frequency and the fast Fourier transform (FFT) is used to convert the sampled time-domain signals to frequency-domain data. It is emphasised that the measured voltages at the receiving antenna output terminals are proportional to the respective electric field intensities at the location of the receiving antenna. Care must be taken to ensure that conditions set during the free-space measurement are as closely identical as possible to

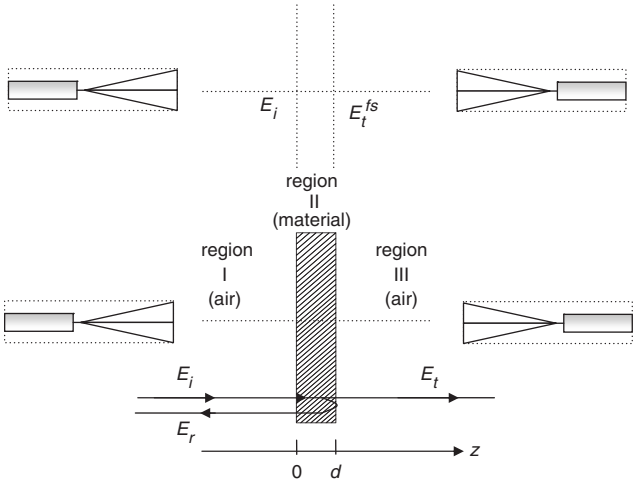

Fig. 1 *Schematic of experiment setup for 'free-space' (in the absence of material layer) and 'through' (material layer in place) measurements*

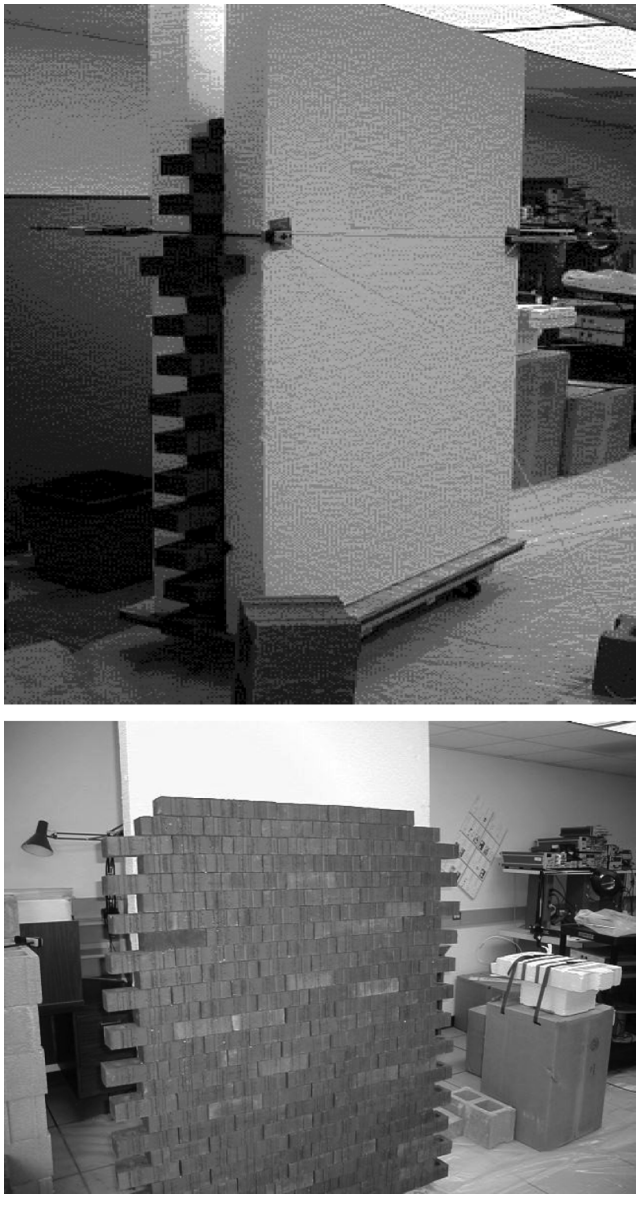

Fig. 2 *Illustration of a constructed moving wall for accurate reference measurements*

those for the measurement when the material slab is in place. It is difficult to perform *in-situ* and free-space measurements under identical conditions. To overcome this challenge, walls were built or mounted on a moving platform to obtain free-space reference and through-the-wall measurements. An example of a moving wall is illustrated in Fig. 2.

To ensure better accuracy in the characterisation of materials, six different measurements are performed for each material. These include four time-domain measurements with two different pairs of antennas and two pulse generators with different pulse waveforms, and two frequency-domain measurements using two pairs of antennas. The first pulse generator provides trapezoidal-shaped pulses with 10-V amplitude and a rise time of 45 ps. The second generator provides Gaussian-like pulses with a 7-V amplitude and a FWHM (full-width half-maximum) duration of 85 ps. In each measurement, two pairs of wideband TEM horn antennas are used. The 3 dB bandwidth for the first pair is 1–7 GHz and for the second pair is 1–12 GHz. Measurements are performed both in the time domain using pulse generators along with a sampling oscilloscope, and in the frequency domain using a vector network analyser.

3 Analysis techniques

The free-space and through-the-wall measurements would be most accurate if performed inside an anechoic chamber where all the multipath components and reflections from the floor and ceiling are absorbed. Ideally, the sample to be measured should be infinitely wide to avoid scattering from the edges. Samples under test have to be at a far-field distance from the antenna, typically several metres for the frequency range of interest and dimensions of the antennas used. Maintaining these requirements is not a convenient task, keeping in mind that absorbers and chamber environment do not allow easy movement of large samples. Fortunately, time gating can be used to reduce significantly the undesired effects, such as reflections from the surrounding walls and scattering from edges. For time gating to be efficiently implemented, three conditions have to be met. First, the transmitter and the receiver antennas should be positioned away from the reflecting surfaces. Secondly, samples should have relatively large surface dimensions in order to minimise the edge effects. Finally, there should be flexibility in adjusting the distance between the antenna and the sample. Time gating can also be used to isolate a desired portion of the received signal; namely, the first-pass of the pulse signal transmitted through the slab. In this application, the sample thickness should be large enough to yield sufficient delay. Thus, not only zooming on and extracting the first-pass pulse, but also removing all delayed pulses due to multiple reflections inside the slab, become possible. In the following Sections, analysis techniques based on single-pass, multiple-pass, and approximate solutions for low-loss materials are presented.

3.1 Single-pass technique

Single-pass technique can be used if the duration of the test pulse is sufficiently short or the wall or material slab under study has a thickness that is large enough to allow elimination, by means of time gating, of the portions of the signal due to multiple reflections inside the slab which are delayed more than the width of the pulse. The same technique can be used to eliminate antenna ringing and extraneous signal components.

3.2 Multiple-pass technique

If the single-pass signal cannot be gated out satisfactorily, multiple reflections from the slab interior that constitute part of the received signal must be considered. This situation particularly arises when the transit time through the thickness of the slab is small compared to the pulse duration. In this case, an insertion transfer function that accounts for multiple reflections is needed. In order to determine the complex dielectric constant from the measured insertion transfer function, a mathematical expression for $H(j\omega)$ is needed. To calculate $H(j\omega)$, it is assumed that an x-polarised uniform plane wave, representing the local far-field of the transmitting antenna is normally incident on a slab of material with thickness d. The material has an unknown complex dielectric constant $\varepsilon_r = \varepsilon_r' - j\varepsilon_r''$. The incident plane wave, as depicted in Fig. 1, establishes a reflected wave in region I (air), a set of forward and backward travelling waves in region II (material) and a transmitted wave in region III (air). Imposing the boundary conditions for the electric and the magnetic fields at the slab–air interfaces, the transmission coefficient can be calculated in a straightforward manner. The result is

$$T = \frac{E_t e^{-j\beta_0 d}}{E_i} = \frac{4}{e^{\gamma d}\left(2 + \frac{\eta_1}{\eta_2} + \frac{\eta_2}{\eta_1}\right) + e^{-\gamma d}\left(2 - \frac{\eta_1}{\eta_2} - \frac{\eta_2}{\eta_1}\right)} \quad (2)$$

where

$$\beta_0 = \omega\sqrt{\mu_0\varepsilon_0} = \frac{2\pi}{\lambda} = \frac{2\pi f}{c}$$

$$\gamma = \alpha + j\beta = j\omega\sqrt{\mu_0\varepsilon_0(\varepsilon_r' - j\varepsilon_r'')}$$

$$\eta_2 = \sqrt{\frac{\mu}{\varepsilon_0(\varepsilon_r' - j\varepsilon_r'')}}$$

$$\eta_1 = \sqrt{\frac{\mu_0}{\varepsilon_0}} = 120\,\pi\,\Omega$$

The insertion transfer function is related to the transmission coefficient by $Te^{j\beta_0 d} = H(j\omega)$. It should also be noted that the transmission coefficient T is equivalent to the scattering parameter S_{21}. In terms of the scattering parameter S_{21}, the parameter that is directly measured, (2) can be cast into the following form:

$$\left(x + \frac{1}{x}\right)\sinh(xP) + 2\cosh(xP) - \frac{2}{S_{21}} = 0 \quad (3)$$

where $x = \sqrt{\varepsilon_r}$, $S_{21}(j\omega) = H(j\omega)e^{-j\omega\tau_0}$, $\tau_0 = c/d$ and $P = j\beta_0 d$. This equation can be solved numerically for the complex dielectric constant $\varepsilon_r = \varepsilon_r' - j\varepsilon_r''$ using two-dimensional search algorithms. For low-loss materials, the complex dielectric constant can be evaluated by means of real equations and one-dimensional root search techniques. The details of this approach are given in [13].

4 Signal processing

Over a given frequency range, 801 complex (magnitude and phase) data points, the maximum number allowed by a vector network analyser, can be collected. This limitation on the number of points imposes a limit on the measurement resolution and the accuracy of transformation to the time domain using the inverse Fourier transform. Zeros are

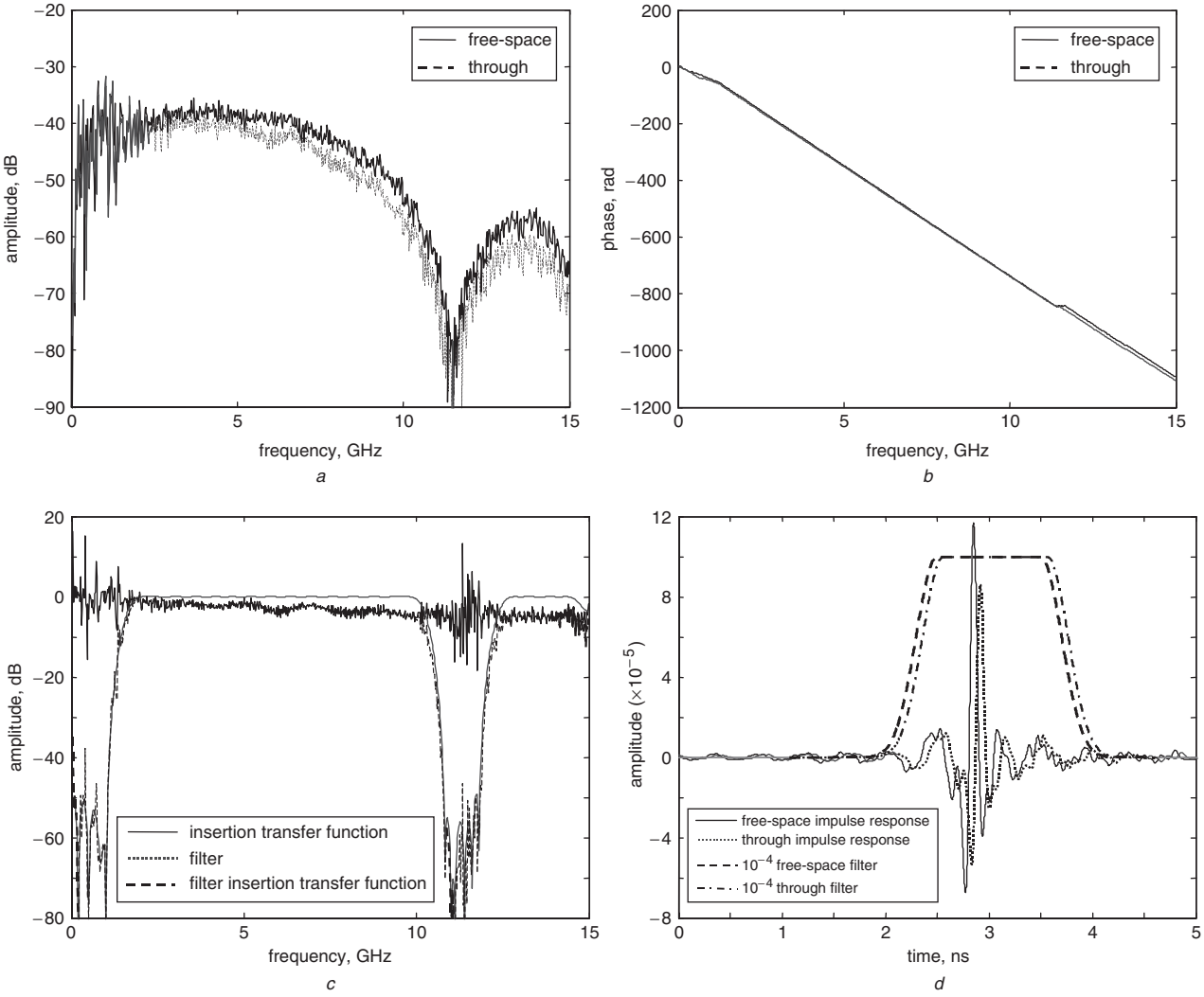

Fig. 3 *Examples of frequency-domain measurements*
a Magnitude of insertion transfer function
b Phase of insertion transfer function
c Filtered and filtered ungated insertion transfer function
d Impulse response and weighted gating window

padded to get higher resolution upon transformation into the time domain. A lowpass FIR (finite-impulse-response) filter is used to remove the noise beyond the antenna bandwidth. The cutoff frequencies of the filter are adjusted to remove noisy regions. A sample frequency-domain measurement is shown in Fig. 3 which illustrates the magnitude and the unwrapped phase of the 'free-space' and 'through' signals, the FIR filter characteristic and the obtained impulse responses.

For time-domain measurements, 128 traces are averaged, each acquired in a 5 ps sampling time using a sampling oscilloscope. Offset adjustment is achieved through load calibration and postprocessing. The window in which the signal is acquired spans more than 10 ns and consists of 2048 points. A typical time-domain measurement is shown in Fig. 4. Note that this measurement clearly shows the line-of-sight signal along with a reflection from the floor.

The 'through' and 'free-space' time-domain measured signals or the corresponding impulse responses obtained from frequency-domain measurements are correlated using a sliding correlator to obtain an initial guess of the delay and effective dielectric constant. An estimate of the average dielectric constant could also be obtained through peak-to-peak impulse time delay $\Delta\tau$. An average value of the

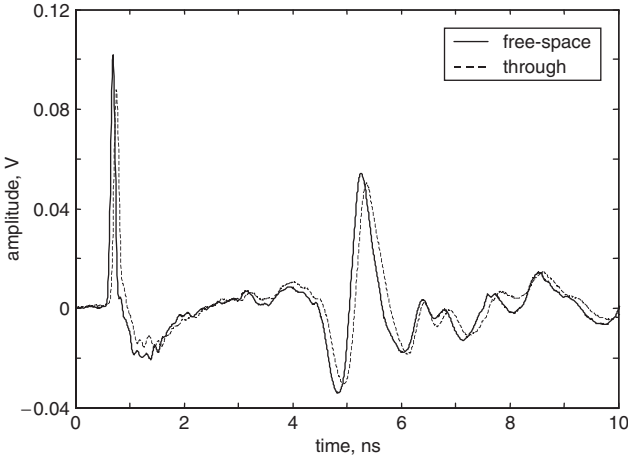

Fig. 4 *Free-space and through sample door time-domain measurements*

dielectric constant that does not contain the frequency dependence is given by

$$\varepsilon_r' \cong \left[1 + \frac{\Delta\tau}{d/c}\right]^2 \tag{4}$$

Time gating is required to remove multipath components from the surrounding walls and scattered fields from the material edges in received signals, as they are not accounted for in calculation and extraction of material parameters. However, perfect time gating cannot be achieved because, strictly speaking, infinite acquisition time is required to capture an infinite number of multiple reflections from the material interior, and the line-of-sight signal might have small overlaps with multipath components and scattered fields from the material edges. However, because higher-order multiple reflections die out quickly for materials of interest, time gating capabilities are enhanced with shorter pulse durations and longer distances between the test material and reflectors and/or scatterers. If single-pass is desired, pulse duration should be shorter than twice the travel time through the slab in order to avoid pulse overlapping.

To avoid abrupt changes in the signal level, the gating-window should have a smooth transition from zero to the flat level. This window is based on the modified Kaiser window with a flat region in the middle. However, the results for material parameters should be essentially independent of the window opening. Various parameters of the window are changed to make sure that the results are not sensitive to the details of the window. If the 'through' and 'free-space' signals both return to the zero level in the window, the gating can be implemented easily. After time gating the signals, fast Fourier transform (FFT) with proper zero padding is utilised and the insertion transfer function is calculated. From the complex insertion transfer function, the dielectric constant (real part of the complex relative permittivity) and loss tangent of the material under test can be extracted. The choice of analysis technique is based on how satisfactorily time gating can be implemented. In many cases, multiple reflections inside the slab decay rapidly so that single-pass and multiple-pass techniques essentially yield the same results.

Confidence in the obtained results is strengthened whenever time-domain and frequency-domain measurements agree well, because different equipment, calibrations and processes are involved in the entire measurement scheme implemented in the two domains. The main advantage for the frequency-domain technique is that no external synchronisation is required. Both input and output signals are centrally processed, thus reducing the synchronisation errors. However, the time-domain measurements offer higher resolution and more data points.

5 Description of samples and wall materials

Ten different wall material samples commonly used in building environments are selected for UWB characterisation. These include drywall, cloth office partition, structure wood, wooden door, plywood, glass, styrofoam, brick wall, concrete block, and reinforced concrete pillar. Table 1 summarises the selected samples and their dimensions. Thickness measurements are carried out by averaging 6–8 repeated measurements in order to achieve better accuracy.

The requirement that 'free-space' and 'through' measurements should be performed with exactly equal antenna separations renders *in-situ* measurements impractical. Because, after *in-situ* 'through' measurements are performed, 'free-space' measurements should be carried out at a different location but with the same distance between the transmitting and receiving antennas as in the 'through' measurement setup. Since it is impossible to have exactly the same distances between the antennas for measurement setups at two different locations, errors will inevitably occur in the calculation of insertion transfer function. To emphasise how large such errors might be, a 10 GHz signal corresponding to a 3 cm free-space wavelength is considered. Only 1 mm change in the spacing between the two antennas would result in 12 degrees of phase error. This fact implies an extremely tight tolerance requirement that cannot be met easily. To overcome this problem, a moving platform as shown in Fig. 2 is used. This allows us to place the wall between the two antennas and make repeated measurements while the setup is kept at a fixed location. Styrofoam slabs were used to support the constructed walls. A single styrofoam slab was subsequently measured to estimate its loss and dielectric constant and hence its impact on the measurement of other materials. It was observed that a styrofoam slab has very low loss and a dielectric constant close to unity, thus it can be safely assumed to be effectively 'air'.

Table 1: Sample building materials and dimensions

Material	Dimensions, cm
Drywall	**1.17** × 121.8 × 196.9
Cloth partition	**5.93** × 140.7 × 153.1
Structure wood	**2.07** × 121.5 × 197.8
Wooden door	**4.45** × 90.70 × 211.8
Plywood	**1.52** × 121.9 × 197.51
Glass	**0.24** × 1.44 × 111.76
Styrofoam	**9.91** × 121.8 × 197.7
Brick	**8.71** × 5.82676 × 19.8
Concrete block	**19.45** × 39.7 × 19.5
Reinforced concrete wall	**60.96** × 121.92 × …

The first number is the thickness of the sample; i.e. the propagation path length through the material

A reinforced concrete pillar in the third floor of Whittemore Hall, the building that houses the Electrical and Computer Engineering Department at Virginia Tech, was measured. Also, a reinforced pillar in the Time Domain Lab (TDL, located in the fourth floor of Whittemore Hall) was measured as a second reinforced concrete sample. The cloth office partitions that were tested have round edges at the upper ends with wooden caps for holding the cloth material tightly. Each partition has two metal stands as well as support pieces inside.

6 Measurement results

For each material four time-domain and two frequency-domain measurements of free-space and through signals are performed. Then, using (1), the insertion transfer function for each measurement is determined. Figure 5 shows the magnitude and phase characteristics of the insertion transfer function for a sample wooden door obtained from the six different measurements. With the insertion transfer function, $H(j\omega)$ or the scattering parameter $S_{21}(j\omega)$, determined, the complex relative permittivity of the material $\varepsilon_r = \varepsilon_r' - j\varepsilon_r''$ is calculated from (3). We also used the method described in [13] to calculate ε_r' and ε_r'', and essentially obtained the same results. Here, the results for the average values of dielectric constant ε_r' and loss tangent $\varepsilon_r''/\varepsilon_r'$ from all measurements are presented.

Figures 6 and 7 illustrate variations of the dielectric constant and loss tangent against frequency for the materials tested. In order to give a measure of accuracy for these results, we compare our data with those available

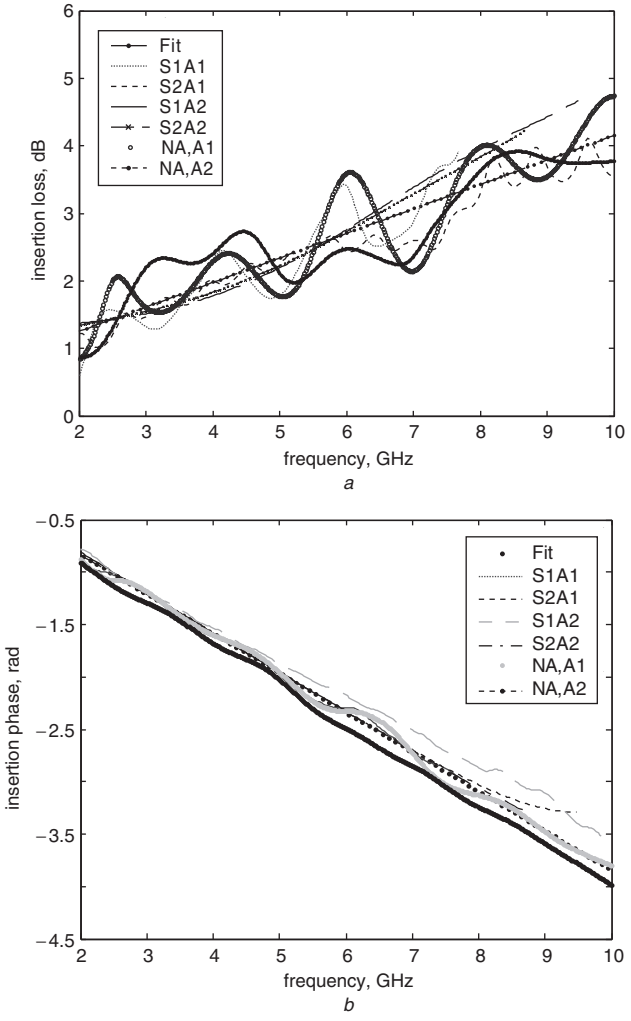

Fig. 5 *Insertion loss against frequency for sample door for four time-domain and two frequency-domain measurements*
a Magnitude (dB)
b Phase (rad)

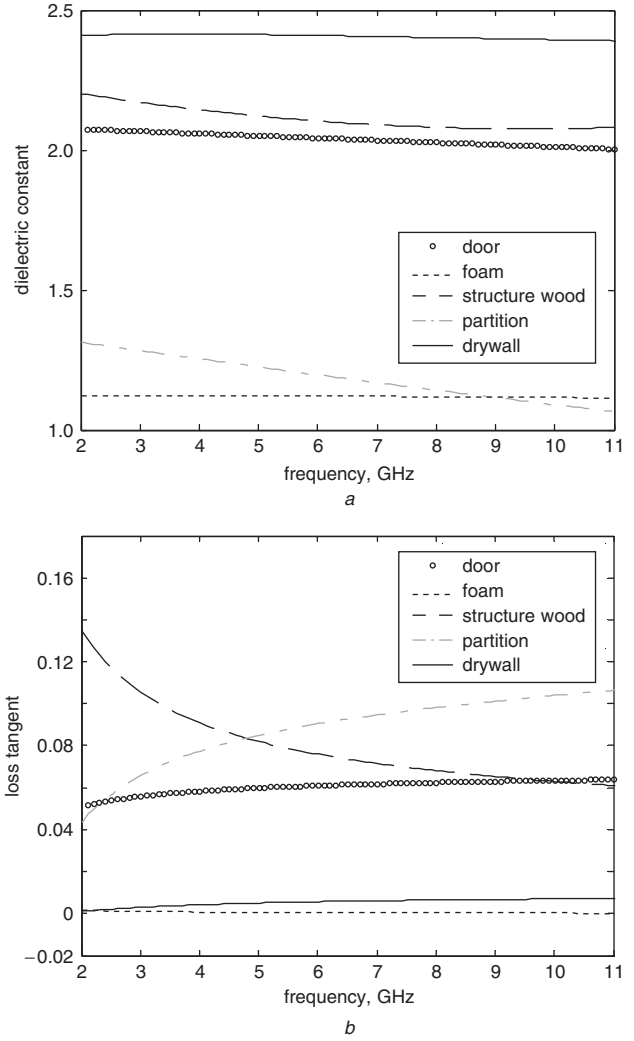

Fig. 6 *Variations of dielectric constant and loss tangent against frequency for wooden door, styrofoam, structure wood, office partition and drywall*
a Dielectric constant
b Loss tangent

in the literature. Landron *et al.* [3] report a value of 4.44 for the dielectric constant of brick at 4.0 GHz, while Suzuki and Mohan [4] have measured the dielectric constant of brick to be $\varepsilon_r' = 4$ at 1 GHz. Our results for the dielectric constant of brick, given in Fig. 7*a*, indicate that $\varepsilon_r' \approx 4$ in the lower frequency range. Cuinas and Sanchez [6] have also measured the dielectric constant of brick at 5.8 GHz. They report a mean value of 3.58 and a maximum of 4.33 for the dielectric constant of brick and a value of 0.11 S/m for its conductivity σ. Again from Fig. 7*a*, a value of about 4.3 is read at 5.8 GHz for the dielectric constant of brick, while from Fig. 7*b* the loss tangent of brick at 5.8 GHz is 0.07, which corresponds to a conductivity of 0.097 S/m. (conductivity and loss tangent are related through the equation $\sigma = \omega\varepsilon_0\varepsilon_r' \tan\delta$). It is noted that our results for the dielectric constant and loss tangent of brick are in general good agreement with the above-mentioned published data. The results of Cuinas and Sanchez [6] for the dielectric constants of glass ($\varepsilon_r' = 6.06$) and plasterboard ($\varepsilon_r' = 2.02$) compare well with our results for glass ($\varepsilon_r' = 6.7$) and drywall ($\varepsilon_r' = 2.4$). Bertoni also provides useful information on the dielectric constant of a number of building materials at selected frequencies [14]. Among these, the dielectric constants of glass, wood and dry brick, at 3 GHz, can be compared with our results for glass, wooden door and brick. From Figs. 6*a* and 7*a*, the values of $\varepsilon_r' = 2.1$ for wooden door, $\varepsilon_r' = 6.7$ for glass and $\varepsilon_r' = 3.9$ for brick at 3 GHz are consistent with $\varepsilon_r' = 1.5$–2.1 for wood, $\varepsilon_r' = 3.8$–8 for glass, and $\varepsilon_r' = 4$ for dry brick reported in [14].

These comparisons clearly indicate that the results for the dielectric constant of materials tested are sufficiently accurate. However, the accuracy of loss tangent, conductivity or ε_r'' is less certain. This uncertainty is also widely reflected in reported data. For example, Suzuki and Mohan [4] report a conductivity of 0.003 for brick, which is vastly different from the value of 0.11 reported by Cuinas and Sanchez [6], and both of these data are significantly different from 0.008–0.016 S/m (corresponding to $\varepsilon_r'' = 0.05$–0.1 at 3 GHz) reported in [14]. Of course, one should bear in mind that the materials of the same category measured by different researchers may not have the same composition, hence differences in their results might indeed be expected. Nonetheless, it is well known that for most materials, measuring the loss is a more difficult task than measuring the real part of the relative permittivity. Because of the very small thickness of our glass sample, no reliable results for the loss tangent of glass could be obtained, and for this reason Fig. 7*b* does not include the loss tangent curve for glass. Overall, we believe that our results for the loss tangent of materials tested are relatively accurate, because they have been obtained from different measurement techniques and with different equipment. It is emphasised that in many situations the insertion loss of a wall is largely due to the

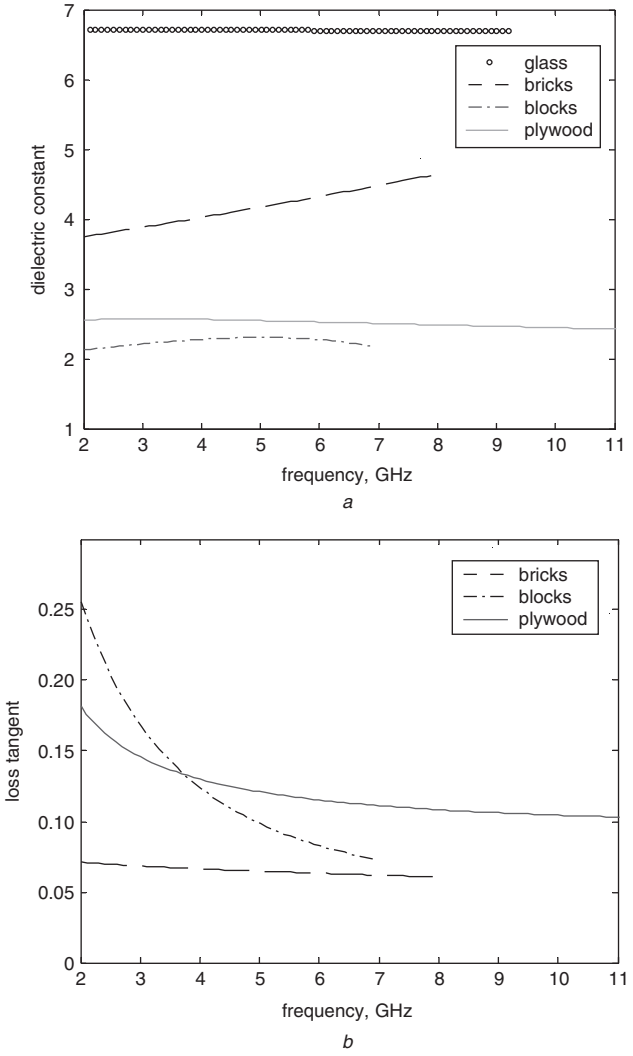

Fig. 7 *Variations of dielectric constant and loss tangent against frequency for glass, brick, concrete block and plywood*
a Dielectric constant
b Loss tangent

reflection and much less due to the absorption of the signal, thus the inaccuracies in loss tangent do not have a major impact on pathloss evaluations.

The materials tested may be divided into two groups; those like drywall, wooden door, structure wood, plywood and glass with uniform structures, and the ones such as brick, concrete block and office partition with nonuniform structures. A close examination of Figs. 6*a* and 7*a* indicates that the dielectric constants of materials with uniform structure, in the average sense, tend to decrease with frequency, whereas the dielectric constants of the materials with nonuniform structure exhibit a more complex behaviour. Particular behaviour of the loss tangent of such materials is also observed. For example, the dielectric constant of brick increases with frequency. The differences in the behaviour of brick, block and partition may be attributed to the fact that, in addition to material properties, their internal structural characteristics also influence the effective dielectric constant.

In order to gain some qualitative understanding on how the structural properties might influence the effective dielectric constant, let us consider a wall consisting of two uniform lossless slabs of dielectric constant ε_r and thickness d separated by a distance w. This wall is modelled as an equivalent uniform slab of total thickness $2d + w$ and effective dielectric constant ε_{eff}. The wall and its equivalent

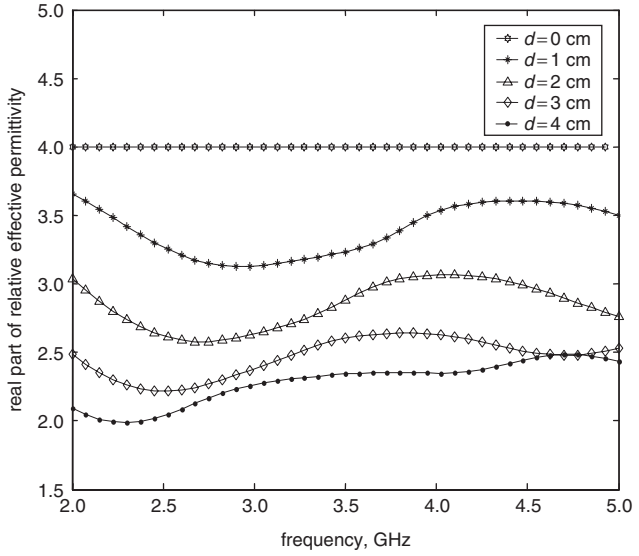

Fig. 8 *Variations of effective dielectric constant against frequency for a nonuniform wall made of two slabs of dielectric constant 4*

yield the same transmitted fields ($\vec{E}^t$, $\vec{H}^t$) for the same incident fields ($\vec{E}^i$, $\vec{H}^i$). The two walls have the same transmission coefficient $T = E^t/E^i$. The transmission coefficient of each wall can be derived by writing the fields in different regions and applying the boundary conditions at air–slab interfaces. For given values of ε_r, d and w, the effective dielectric constant of the equivalent wall can be determined. Figure 8 illustrates variations of the real part of ε_{eff} against frequency for $\varepsilon_r = 4$, $w = 2.2$ cm and several values of d. These results clearly demonstrate the influence of the structural features of a nonuniform wall on the effective dielectric constant. In particular, it is observed that, for example, for $d = 4$ cm the effective dielectric constant tends to increase with frequency. This behaviour is consistent with that of the brick wall measured in this work.

The reinforced concrete wall resulted in a very small amount of received power. No further processing could be performed, but an average dielectric constant of $\varepsilon_r = 9.2$ was obtained by measuring the time delay between the incident and received pulses. For reinforced concrete, concrete block and brick walls, an amplifier with 10 dB gain and 15 GHz bandwidth was used at the receiver side to increase the measured signal level. For the styrofoam, the measured insertion loss was very small, thus the loss tangent for this material is virtually zero.

The distance between the sample and the antenna should be large enough to ensure that the sample is in the far-field of the antenna. However, as the distance increases the signal level decreases and, hence, the frequency range over which reliable characterisation can be achieved becomes smaller. Most of our measurements were performed with a total distance of 1–3 m. An experiment was performed by varying the distance between the antennas and the sample in steps of 0.25 m. No significant changes in the results, other than minor variations in signal levels, were observed.

The thickness of the layer or wall to be characterised is a critical parameter. If the thickness is very small, errors become more pronounced. For example, to estimate the dielectric constant of a slab of glass of 2 mm thickness, one should be able to measure the delay occurring when the incident signal permeates this thin layer. If the thickness is larger, there will be longer delays to measure, and hence less error will occur. However, very thick slabs may cause high losses, resulting in weak signal levels that cannot be accurately measured. For the case of glass samples, slabs

consisting of one, two and three layers were tested to confirm the obtained parameters. The layers were carefully aligned to reduce the air gap. For the case of the drywall, two layers were tested to confirm the results.

7 Signal distortion

When propagating through walls, UWB signals suffer more severe degradations than narrowband signals, because of the effects of frequency-dependent dielectric constants of wall materials in the propagation paths. In narrowband signals, the entire spectrum travels with the same speed and suffers the same attenuation, thus there is no material dispersion effect. However, in ultrawideband cases, each spectral component of the signal undergoes a different amount of delay and suffers a different amount of attenuation, because the complex dielectric constant varies with frequency. This was the prime motivation for the UWB characterisation of building materials presented here.

To appreciate the significance of signal distortion in UWB applications, let us first examine the propagation of a short bipolar Gaussian pulse through a brick wall and a door. This problem can be treated using the transmission-line method in conjunction with the Fourier and inverse Fourier transforms. The waves incident on and refracted from the wall are assumed to be plane waves. The effects of transmitting and receiving antennas are not included in the simulation. The distance between the wall and either antenna is assumed to be large enough such that the plane-wave assumption holds. The brick wall and the door are the same as those used in the measurements discussed in Sections 5 and 6. Figures 9*a* and 9*b* compare the free-space transmission with transmitted signals through the brick wall and the door, respectively. The signal transmitted through the brick wall has suffered significant distortions, whereas the signal transmitted through the door, apart from some loss, has largely maintained its shape. For brick, as noted before, the dielectric constant (ε_r') varies more strongly with frequency than the dielectric constant of the door. This, together with the larger thickness of the brick wall compared to that of the door, causes the transmitted signal through the brick wall to become more severely distorted than the signal transmitted through the door.

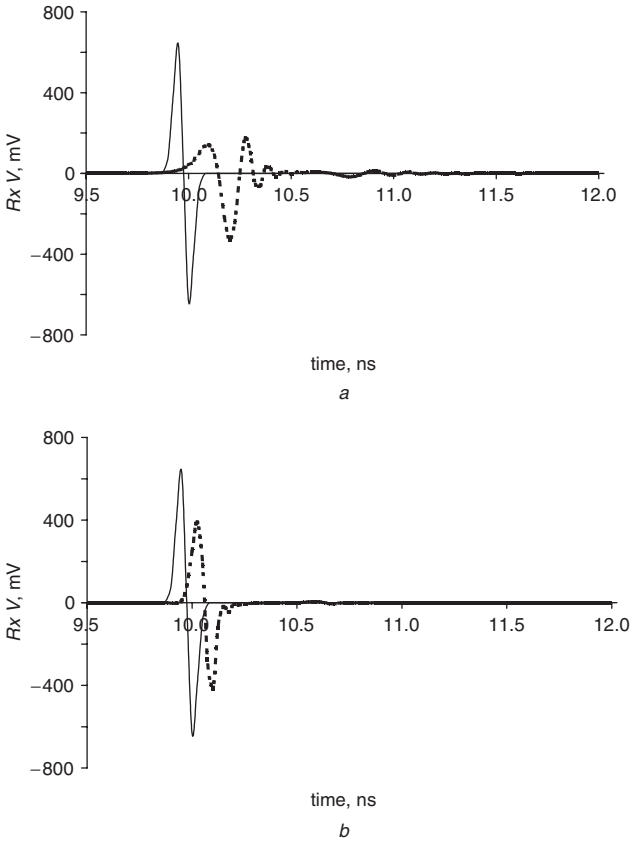

Fig. 9 *Comparison of free-space (solid line) and through-wall (dashed line) transmissions*
a Brick wall
b Wooden door

8 Conclusions

The electromagnetic characterisation of common building materials and walls was undertaken with the aim of assessing their impacts on UWB signal propagation in indoor environments. Ten materials, including drywall, plywood, structure wood, wooden door, glass, brick wall, concrete block wall, styrofoam, office cloth partition and reinforced concrete wall, were examined. Measurements were carried out in both time domain and frequency domain as well as with different antennas and pulse generators. Also, as far as possible, we compared our results with those reported in the literature. Generally, the results for the real part of the complex relative permittivity (ε_r') agree well with the available published results. However, there is less certainty of the accuracy of the imaginary part of the complex relative permittivity (ε_r''). Also, signal distortions due to dispersive properties of walls were demonstrated. The presented results may be used in further studies aimed at developing channel models for UWB wireless communication systems. The results are also very useful for pathloss assessment and in UWB link budget analysis.

9 References

1 Hashemi, H.: 'The indoor radio propagation channel', *Proc. IEEE*, 1993, **81**, pp. 943–968
2 Zhang, Y.P., and Hwang, Y.: 'Measurements of the characteristics of indoor penetration loss'. IEEE 44th Vehicular Technology Conf., 1994, Vol. 3, pp. 1741–1744
3 Landron, O., Feuerstein, M.J., and Rappaport, T.S.: 'A comparison of theoretical and empirical reflection coefficients for typical exterior wall surfaces in a mobile radio environment', *IEEE Trans. Antennas Propag.*, 1996, **44**, (3), pp. 341–351
4 Suzuki, H., and Mohan, A.S.: 'Measurement and prediction of high spatial resolution indoor channel characteristic map', *IEEE Trans. Veh. Technol.*, 2000, **49**, (4), pp. 1321–1333
5 Kharkovsky, S.N., Hasar, U.C., Akay, M.F., and Atis, C.D.: 'Measurement and monitoring of microwave reflection and transmission properties of cement based materials for propagation modelling'. Proc. 53rd Vehicular Technology Conf., 2001, Vol. 2, pp. 1202–1206
6 Cuinas, I., and Sanchez, M.G.: 'Measuring, modeling, and characterization of indoor radio channel at 5.8 GHz', *IEEE Trans. Veh. Technol.*, 2001, **50**, (2), pp. 526–535
7 Pena, D., Feick, R., Hristov, H.D., and Grote, W.: 'Measurement and modeling of propagation losses in brick and concrete walls for the 900-MHz band', *IEEE Trans. Antennas Propag.*, 2003, **51**, (1), pp. 31–39
8 Mazurin, O.V., and Streltsina, M. V.: 'Handbook of glass data, Part A: Silica glass and binary silicate glasses' (Elsevier, New York, USA, 1983)
9 Torgivnikov, G.I.: 'Dielectric properties of wood and wood-based materials' (Springer–Verlag, USA, 1993)
10 Daniels, D.J.: 'Surface-penetrating radar' (IEE, UK, 1996), p. 33
11 Afsar, M.N., Birch, J.R., and Clarke, R.N.: 'The measurement of the properties of materials', *Proc. IEEE*, 1986, **74**, (1), pp. 183–199
12 Baker-Jarvis, J. *et al.*: 'Dielectric characterization of low-loss materials: a comparison of techniques', *IEEE Trans. Dielectr. Electr. Insul.*, 1998, **5**, (4), pp. 571–577
13 Muqaibel, A.H., and Safaai-Jazi, A.: 'A new formulation for characterization of materials based on measured insertion transfer function', *IEEE Trans. Microw. Theory Tech.*, 2003, **51**, (8), pp. 1946–1951
14 Bertoni, H.L.: 'Radio propagation for modern wireless systems' (Prentice Hall PTR, NJ, USA, 2000), p. 55